

Chapter 1

Observations

AU Mic was observed with ALMA on three dates: 26 March 2014, 18 August 2014, and 24 June 2015. All observations were configured with four spectral windows, and employed ALMA’s 12m antennas and Band 7 receivers. Within each observation AU Mic was observed in seven-minute segments.¹ One spectral window was centered around the CO $J = (2 - 1)$ transition at a frequency of 230.538001 GHz, with a total bandwidth of 1.875 GHz and a channel spacing of 488 kHz. The remaining three spectral windows were configured to detect continuum emission with central frequencies of 228.5, 213.5, and 216.0 GHz, total bandwidths of 2 GHz, and channel spacings of 15.6 MHz.

¹Extraneous?

Table 1.1: Observation Information

	26 March 2014	18 August 2014	24 June 2015
Antennas:	32	35	37
Baselines (m):	14–437	20–1268	30–1431
On-source time (min):	35	35	33
Flux calibrator:	Titan	J2056-472	Titan
Bandpass calibrator:	J1924-2914	J2056-4714	J1924-2914
Phase calibrator:	J2101-2933	J2101-2933	J2056-3208
pwv (mm):	0.6	1.6	0.7

Table 1.2: Subtracted point-source fluxes

Time (UTC)	Point-source Flux (μJy)
03:45:0–04:20:0 (no flare)	$(4.1 \pm 0.2) \times 10^2$
4:23:38–4:24:00	$(9.2 \pm 1.7) \times 10^2$
4:24:00–4:25:00	$(1.146 \pm 0.010) \times 10^4$
4:25:00–4:26:00	$(3.59 \pm 0.10) \times 10^3$
4:26:00–4:27:00	$(1.58 \pm 0.10) \times 10^3$
4:27:00–4:28:00	$(4.50 \pm 1.0) \times 10^2$
4:28:00–4:29:00	$(4.60 \pm 1.0) \times 10^2$
4:29:00–4:29:58	$(5.20 \pm 1.0) \times 10^2$

Information regarding the three observation dates can be found in Table 1.1. The short-baseline March observation provides information about AU Mic’s disk on large spatial scales; in contrast, the subsequent long-baseline August observation was intended to trace the small-scale structure of the disk. The quality of the gain transfer for the August observation was tested using observations of the quasar J2057-3734. Due to subpar² quality, the August data were supplemented with a second night of long-baseline observations in June 2015. The quasar J2101-2933 was used to assess the gain transfer quality. During the last segment of the June observation (04:23:38-04:29:58 UT), the host star flared. While we initially fit and subtracted off the flare fluxes (see Table 1.2), it was ultimately decided that the data taken during the flare was too problematic to be included in our analysis.

Calibration, reduction, and imaging were carried out using the **CASA** and **MIRIAD** software packages. Standard ALMA reduction scripts were applied to the datasets: phase calibration was accomplished via water vapor radiometry tables, and system temperature calibrations were performed to account for variations in instrument and weather conditions. Flux and bandpass calibrations were subsequently applied.

²too informal?

Table 1.3: Imaging Parameters for AU Mic

Weighting Scheme	Beam Size (")	Beam PA (°)	RMS Noise (μ Jy)
Natural (no taper)	blank	blank	blank
Natural (200 k λ)	blank	blank	blank

The authors travelled to the NRAO facility in Charlottesville, VA in October 2015 to further process the data in **CASA**. For each observation, an elliptical gaussian was fit with the task **imfit** to a small region around the star in the sky plane (for the June date, the flare data were excluded). The equatorial coordinates of the the model gaussian centroid were then used to define the star position, which was uncertain due to AU Mic’s high proper motion: each dataset was phase shifted using the task **fixvis** so that the pointing center of the data was the same as the fitted star position.

Imaging was performed via standard Fourier inversion using the **CASA** task **tclean**. Two weighting schemes were used: (i) natural weighting with no taper, to trace the small-scale disk structure and (ii) natural weighting with a 200 k λ Gaussian taper applied to long baselines, to bring out the disk emission on larger spatial scales. Because the **CASA** task **tclean** preserves pointing center offsets when converting several visibility datasets into an image, it was necessary to combine the data into a single file before cleaning in order to account for the offset in phase center between datasets. This was done using the task **concat**, which combines datasets with pointing centers aligned so long as their pointing centers do not differ by a value greater than the parameter **dirtol** (set to a value of 2").

Chapter 2

Results

AU Mic's disk is resolved in both the radial and vertical directions by the ALMA observations. The disk extends a distance of ~ 40 au on either side of the host star, although the NW side appears to reach slightly further radial extents than the SE side (2.1). However, we are not able to detect the PA offset described by Boccaletti et al. (2015)

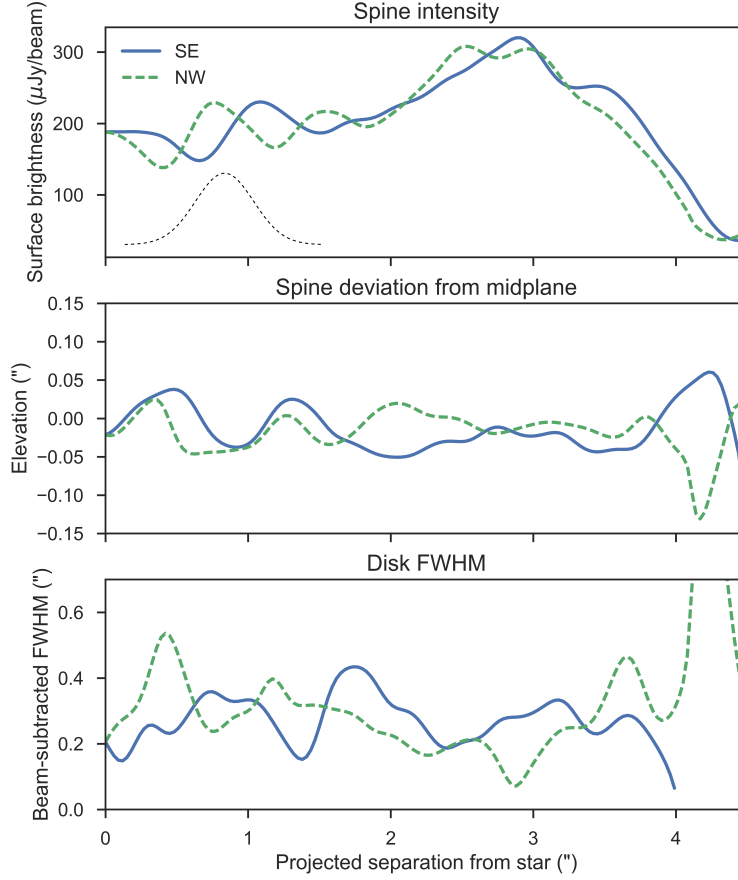


Figure 2.1: Image-domain analysis of AU Mic’s radial structure. At each radial location along the disk midplane, a 1-D Gaussian was fit to the vertical surface brightness profile at that location. From top to bottom, the three plots show the amplitude, centroid and width of the Gaussian fit as a function of angular separation from the star. The Gaussian traced by the dotted line in the upper pane shows the width of the synthesized beam in the radial direction. In the bottom pane, the broadening effects of the synthesized beam in the vertical direction have been removed; the fact that the image-domain vertical height of the disk is in excess of the beam contribution implies that our data spatially resolve the vertical structure of the disk.

Chapter 3

Analysis

1. Describe model & model pipeline
2. weighting goes here?

Testing!

Bibliography

Boccaletti, A., Thalmann, C., Lagrange, A.-M., et al. 2015, *Nature*, 526, 230